

Complex oxide with negative thermal expansion for producing ceramic matrix composites with invar effect

Cite as: AIP Conference Proceedings **1783**, 020037 (2016); <https://doi.org/10.1063/1.4966330>
Published Online: 10 November 2016

Elena S. Dedova, Mariya U. Pertushina, Anton I. Kondratenko, Mikhail V. Gorev, and Sergei N. Kulkov



View Online



Export Citation

ARTICLES YOU MAY BE INTERESTED IN

Synthesis conditions and sintered ZrW_2O_8 structure

AIP Conference Proceedings **1783**, 020036 (2016); <https://doi.org/10.1063/1.4966329>

Ultra-low thermal expansion realized in giant negative thermal expansion materials through self-compensation

APL Materials **5**, 106102 (2017); <https://doi.org/10.1063/1.4990481>

Composites with extremal thermal expansion coefficients

Applied Physics Letters **69**, 3203 (1996); <https://doi.org/10.1063/1.117961>



Your Qubits. Measured.

Meet the next generation of quantum analyzers

- Readout for up to 64 qubits
- Operation at up to 8.5 GHz, mixer-calibration-free
- Signal optimization with minimal latency

[Find out more](#)



Complex Oxide with Negative Thermal Expansion for Producing Ceramic Matrix Composites with Invar Effect

Elena S. Dedova^{1,2,3,a)}, Mariya U. Pertushina^{4,b)}, Anton I. Kondratenko^{3,c)},
Mikhail V. Gorev^{5,d)}, and Sergei N. Kulkov^{1,2,3,e)}

¹ *Institute of Strength Physics and Materials Science SB RAS, Tomsk, 634055 Russia*

² *National Research Tomsk State University, Tomsk, 634050 Russia*

³ *National Research Tomsk Polytechnic University, Tomsk, 634050 Russia*

⁴ *Novosibirsk State University, Novosibirsk, 630090 Russia*

⁵ *Kirensky Institute of Physics SB RAS, Krasnoyarsk, 660036 Russia*

^{a)} Corresponding author: lsdedova@yandex.ru

^{b)} mapet1003@mail.ru

^{c)} tid@sibmail.com

^{d)} gorev@iph.krasn.ru

^{e)} kulkov@ms.tsc.ru

Abstract. The article investigates the phase composition of $(\text{Al}_2\text{O}_3-20\text{ wt}\% \text{ZrO}_2)\text{-ZrW}_2\text{O}_8$ ceramic composites obtained by cold-pressing and sintering processes. Using X-ray analysis it has been shown that composites mainly have monoclinic modification of zirconium dioxide and orthorhombic phase of aluminum oxide. After adding zirconium tungstate the phase composition of sintered ceramics changes, followed by the formation of tungsten-aluminates spinel such as $\text{Al}_x(\text{WO}_y)_z$. It has been shown that thermal expansion coefficient of material decreases approximately by 30%, as compared with initial ceramics.

Keywords: ceramics, zirconium tungstate, negative thermal expansion coefficient, phase transformation, spinel

INTRODUCTION

Ceramics is one of the priority groups of materials for creating composites that can be used in extreme conditions [1]. High potential of ceramics is associated with such properties as high temperature stability, corrosion resistance, etc. [2]. However, ceramics like other materials undergo changes in its size when exposed to temperature, which cannot but limit their applications in many industries.

One of the most promising ways to create a new class of ceramic materials is to add to their composite such components that have special thermal expansion coefficient (CTE), i.e. material with small or negative CTE. In order to implement this approach one can add zirconium tungstate which has negative CTE ($\alpha = -9 \times 10^{-6} \text{ }^\circ\text{C}^{-1}$) in a wide temperature range from -273 to 770°C [3, 4].

Unfortunately, there is a lack of research aimed at establishing the structure and the phase equilibrium in these composites, therefore, the question of relationship between the structure and properties of composites still remains open. For example, there are many investigations devoted to zirconia, zirconia-alumina systems [5] and ZrW_2O_8 powders [6] but there is almost no information about $(\text{ZrO}_2-20\text{ vol}\% \text{Al}_2\text{O}_3)\text{-ZrW}_2\text{O}_8$ composites.

The goal of this paper is to investigate the structure, phase transformations and thermal properties of $\text{ZrO}_2\text{-Al}_2\text{O}_3\text{-ZrW}_2\text{O}_8$ oxide system.

MATERIALS AND EXPERIMENTAL PROCEDURES

A mixture of nanocrystalline powders of zirconia with 20 vol % aluminum oxide (TOSOH, Japan) and nanopowder of zirconium tungstate produced by hydrothermal method [6] was used as initial components. The content of zirconium tungstate in the initial mixture was equal to 10, 25, and 55 wt %.

According to SEM, $\text{ZrO}_2(\text{Y}_2\text{O}_3)\text{-Al}_2\text{O}_3$ powder was designated by dense spherical particles, shown in Fig. 1a. The average size of agglomerates was equal to 80 μm with unimodal size distribution. The phase composition of the powder mixture was represented by tetragonal and monoclinic phases of zirconium dioxide and aluminum oxide.

Zirconium tungstate powder had single and interlocked needle-like particles (Fig. 1b). The average transverse size of particles was equal to 0.2 μm . The longitudinal size varied from 0.5 to 5 μm . The phase composition was represented by cubic modification of ZrW_2O_8 [3, 6].

The initial powders were mixed in the AGO-2 planetary mill for 1 min to evenly distribute particles of zirconium tungstate in the powder mixture. Mixing was carried out in drums with ceramic inserts using corundum grinding ball media. As a result of the mixing process, zirconium dioxide granules were decomposed and the final mixed powder was made up of irregularly shaped agglomerates ($d = 31 \mu\text{m}$), a fine powder and needle-like particles of zirconium tungstate (Fig. 1c).

Ceramics $(\text{ZrO}_2\text{-Al}_2\text{O}_3)\text{-ZrW}_2\text{O}_8$ was produced by uniaxial cold pressing in steel molds ($d = 7 \text{ mm}$) at 10 MPa, followed by sintering in high-temperature muffle furnace Nabertherm LHT 02/17 at 1200°C for 1 hour.

The phase composition of the initial powders and composites was studied using diffractometer with $\text{CuK}\alpha$ radiation with step-by-step exposition and time for obtaining statistics accuracy better than 0.5%. Quantitative phase analysis was carried out by determining the ratio of the total integral peaks area of each phase to the total integral area of all diffraction peaks.

The morphology of the powders and the ceramic structure was analyzed by optical microscopy, scanning electron microscopy (SEM) with the Vega Tescan 3SBH microscope and transmission electron microscopy (TEM) with the JEM-2100 device. A random linear intercept method was used to determine the particle size. The dilatometer investigation was conducted using the DEL 402 C DIL 402 C (env.—argon, temperature changed from -170 to 500°C). The thermal expansion coefficient of ceramics was defined as the slope of $\Delta L/L_0\text{-}T$ dependence and compared with values calculated by using the mixture rule $\alpha = \sum \alpha_i V_i$, where α_i is thermal expansion coefficient and V_i is component volume concentration.

RESULTS AND DISCUSSION

Powder diffraction patterns of sintering ceramic composites with different contents of zirconium tungstate are shown in Fig. 2. The phase composition of $\text{ZrO}_2\text{-}20\% \text{ Al}_2\text{O}_3$ sintered ceramics was mainly represented by high-temperature tetragonal modification of zirconium dioxide ($t\text{-ZrO}_2$) and rhombohedral phase of aluminum oxide. There are small (-111) and (111) peaks of monoclinic ZrO_2 ($m\text{-ZrO}_2$) phase [7, 8]. Calculations of phase contents based on X-ray data show that the phase composition coincides with the initial phase contents of powders.

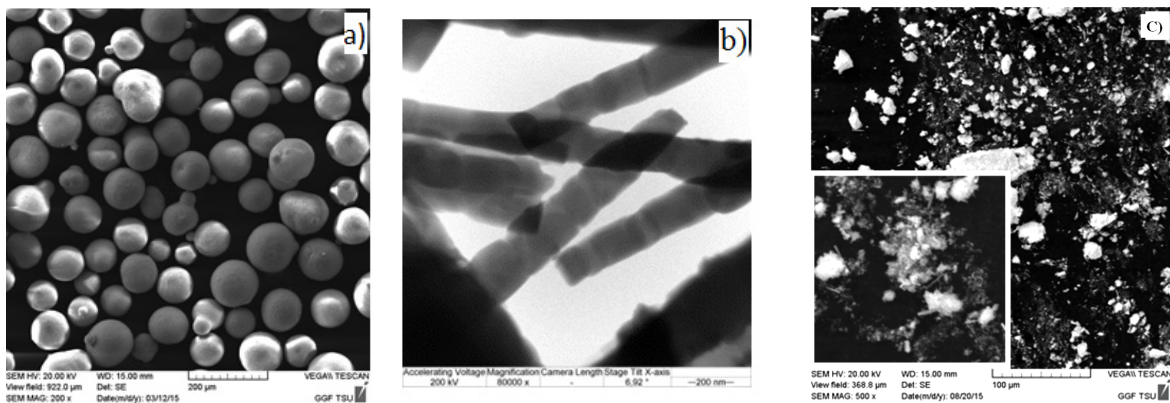


FIGURE 1. SEM image of (a) the $\text{ZrO}_2(3 \text{ mol } \% \text{ Y}_2\text{O}_3)\text{-Al}_2\text{O}_3$, (b) the ZrW_2O_8 , (c) mixture after 1-minute activation in a ball-mill

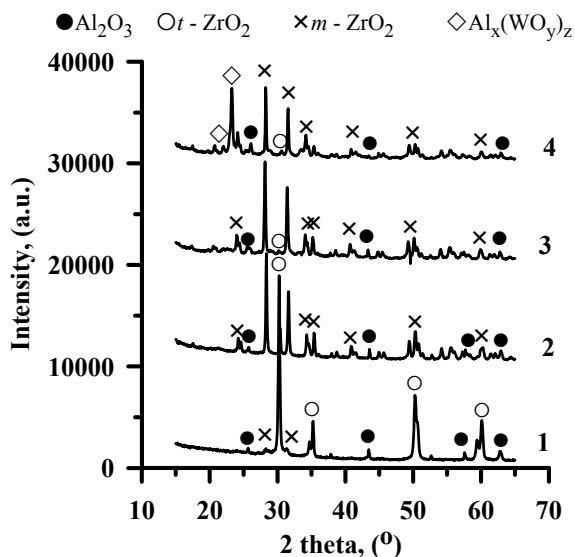


FIGURE 2. Powder diffraction patterns of (ZrO₂-20% Al₂O₃)-ZrW₂O₈ sintering ceramics. Content of ZrW₂O₈: 0 (1), 10 (2), 25 (3), 55 wt % (4)

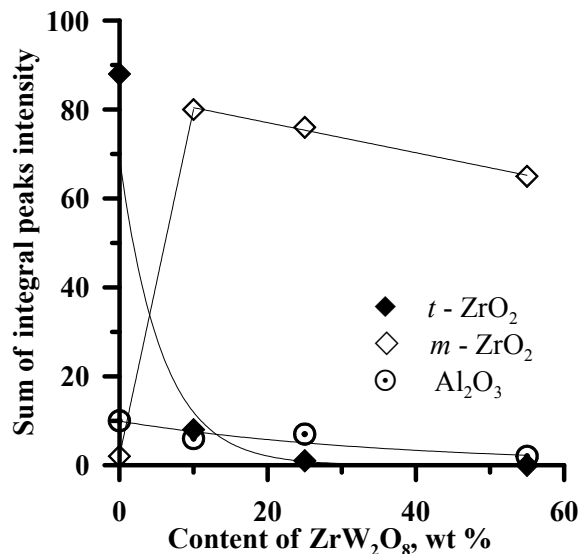


FIGURE 3. The dependence of sum of integral peaks intensity of phases on ZrW₂O₈ content

The addition of zirconium tungstate into the powder mixture led to the change in the phase composition of sintered ceramics: the diffraction pattern of (ZrO₂-20% Al₂O₃)-10 wt% ZrW₂O₈ composite exhibited reflexes of monoclinic ZrO₂ and orthorhombic phase of aluminum oxide and peaks of tetragonal ZrO₂ with low intensity. The content of tetragonal phase of zirconia decreased to 8%. Peaks of zirconium tungstate were not recorded, as shown in Fig. 3, which probably means that ZrW₂O₈ was decomposed into separate oxides [1, 2, 9]. The diffraction patterns of samples with 55% ZrW₂O₈ show peaks of monoclinic zirconium dioxide and Al_x(WO_y)_z (AlWO₄ and Al₂(WO₄)₃) spinels.

It is well known that ZrW₂O₈ is stable up to 770°C [9, 10]. The further temperature increase results in the decomposition of the compound into component oxides—ZrO₂ and WO₃. According to ZrO₂-WO₃ constitutional diagram [11], zirconium tungstate should be re-synthesized at a temperature higher than 1150°C. According to our XRD data, this process is not observed. This may be caused by the evaporation of WO₃ at 1000°C [3, 4] and the reaction between Al₂O₃ and WO₃ that are generated after the decomposition of ZrW₂O₈, with the formation of Al_x(WO_y)_z spinels [12]. Therefore, the addition of zirconium tungstate in ceramics brought about a drastic change in the phase content of ZrO₂ with an increase in monoclinic phase of zirconia.

Nevertheless, according to dilatometer studies, zirconium tungstate affects the thermal properties of ceramics. The dependence of relative elongation of samples on the change in temperature is presented in Fig. 4. The relationship obtained for composites can be divided into two stages with different slope, which describe various values of CTE. For the first range the value of CTE was $\alpha = 6.3$ to $3.5 \times 10^{-6} \text{ }^\circ\text{C}^{-1}$ and for the second area— 5.7 to $9.6 \times 10^{-6} \text{ }^\circ\text{C}^{-1}$. Composites containing 10 wt % ZrW₂O₈ showed the smallest value of CTE (α) = $5.4 \times 10^{-6} \text{ }^\circ\text{C}^{-1}$.

The measured CTE values do not coincide with calculations made by using mixture-rule that should be up to $-0.45 \times 10^{-6} \text{ }^\circ\text{C}^{-1}$ for material with 55 wt % of ZrW₂O₈. On the contrary, for ceramic ZrO₂-20% Al₂O₃ they turned out to be in a good agreement. The observed differences are caused by phase transformations and new phases formed in the course of composite sintering.

CONCLUSION

The phase composition of ZrO₂-20% Al₂O₃ sintered ceramics was mainly represented by tetragonal modification of zirconium dioxide and rhombohedral phase of aluminum oxide. The content of Al₂O₃, ZrO₂ tetragonal phase and ZrO monoclinic phase calculated from X-ray data was equal to 20, 78 and 2%, respectively.

The addition of zirconium tungstate led to the change in the phase composition of sintered ceramics, followed by the formation of 80% monoclinic phase of zirconia.

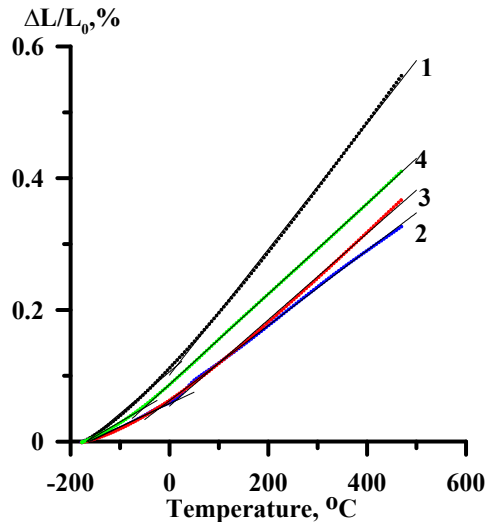


FIGURE 4. The dependence of thermal expansion of samples on temperature: 0 (1), 10 (2), 25 (3), 55 wt % of ZrW_2O_8 (4)

It has been shown that during the sintering process, zirconium tungstate is likely to have been decomposed into component oxides— ZrO_2 and WO_3 . The increase of zirconium tungstate content resulted in the disappearance of aluminum oxide and the formation of $Al_x(WO_y)_z$ spinels. The latter is associated with the interaction between aluminum oxide and tungsten oxide generated after the thermal decomposition of ZrW_2O_8 during the sintering process.

The addition of zirconium tungstate affected the thermal expansion of sintered ceramics. There is a reduction in the thermal expansion of ceramic composite materials by 30%, compared with ZrO_2 –20% Al_2O_3 ceramics.

ACKNOWLEDGMENT

The research was conducted with partial financial support by an agreement with the Ministry of Education No. 14.575.21.0040 (RFMEFI57514X0040). Authors are grateful to Institute of Physics for their help in the dilatometer investigation.

REFERENCES

1. L. Sun, A. Sneller, and P. Kwon, *Compos. Sci. Technol.* **68**, 3425–3430 (2008).
2. K. Takenaka, *Sci. Technol. Adv. Mater.* **13**, 013001 (2011).
3. J. S. O. Evans, *Roy. Soc. Chem. Dalton Trans.*, 3317–3326 (1999).
4. A. W. Sleight, *Ann. Rev. Sci.* **28**, 29–43 (1998).
5. S. P. Buyakova and S. N. Kul'kov, *Inorganic Mater.* **46**(10), 1155–1158 (2010).
6. A. I. Gubanov, E. S. Dedova, P. E. Plyusnin, et al., *Thermochimic. Acta.* **597**, 19–26 (2014).
7. E. S. Dedova, V. S. Shadrin, et al., *IOP Mater. Sci. Eng.* **116**, 020036 (2015).
8. J. F. Bartolomé, A. Smirnov, H.-D. Kurland, J. Grabow, and F. A. Müller, *Sci. Rep.* **6**, 20589 (2016).
9. T. A. Mary, J. S. O. Evans, T. Vogt, and A. W. Sleight, *Science* **272**, 90–92 (1996).
10. K. Kanamori, T. Kineri, et al., *J. Mater. Sci.* **44**, 855–860 (2009).
11. L. L. Y. Chang, M. G. Scroger, B. Phillips, *J. Am. Chem. Soc.* **50**, 385–390 (1967).
12. S. N. Achary, G. D. Mukherjee, and A. K. Tyagi, *J. Mater. Sci.* **37**, 2501 (2002).